# Concurrent and Continuous Prediction of Finger Kinetics and Kinematics via Motoneuron Activities

Rinku Roy, Yang Zheng, Derek G. Kamper, and Xiaogang Hu

Abstract—Objective: Robust neural decoding of intended motor output is crucial to enable intuitive control of assistive devices, such as robotic hands, to perform daily tasks. Few existing neural decoders can predict kinetic and kinematic variables simultaneously. The current study developed a continuous neural decoding approach that can concurrently predict fingertip forces and joint angles of multiple fingers. Methods: We obtained motoneuron firing activities by decomposing high-density electromyogram (HD EMG) signals of the extrinsic finger muscles. The identified motoneurons were first grouped and then refined specific to each finger (index or middle) and task (finger force and dynamic movement) combination. The refined motoneuron groups (separate matrix) were then applied directly to new EMG data in realtime involving both finger force and dynamic movement tasks produced by both fingers. EMG-amplitude-based prediction was also performed as a comparison. Results: We found that the newly developed decoding approach outperformed the EMG-amplitude method for both finger force and joint angle estimations with a lower prediction error (Force: 3.47±0.43 vs 6.64±0.69% MVC, Joint Angle: 5.40±0.50° vs 12.8±0.65°) and a higher correlation (Force: 0.75±0.02 vs 0.66±0.05, Joint Angle: 0.94±0.01 vs 0.5±0.05) between the estimated and recorded motor output. The performance was also consistent for both fingers. Conclusion: The developed neural decoding algorithm allowed us to accurately and concurrently predict finger forces and joint angles of multiple fingers in real-time. Significance: Our approach can enable interactions with assistive robotic hands, and allow the performance of dexterous hand skills involving both force control tasks and dynamic movement control tasks.

Index Terms: Neural decoding, Hand function, Isometric force, Dynamic movement

### I. Introduction

DEXETEROUS control of hand motion is essential to our daily life. In recent years, advanced assistive robotic hands, such as prosthetic hands [1] or exoskeleton gloves [2, 3], have been developed that allow restoration of independent control of individual digits. These devices can be interfaced using neural signals from the brain [4], muscles [5], or peripheral nerves [6]. In particular, these studies have decoded neural signals for hand gesture recognition [4-6]. Despite

This work was supported in part by the National Science Foundation CBET-1847319 and IIS-2106747, and by NIDILRR ARHF19000021. Rinku Roy (email: rroy2@ncsu.edu) and Derek Kamper (email: dgkamper@ncsu.edu) are with the Joint Department of Biomedical Engineering at University of North Carolina-Chapel Hill and NC State University. Yang Zheng (email: yzheng@mail.xjtu.edu.cn) is with the

exciting progress, continuous decoding of individual finger movements from neural signals remains a substantial challenge [7, 8]. Even though neural signals obtained through invasive methods have shown success in detecting finger kinematics and kinetics [9, 10], their wide clinical use has been limited, partly because of the invasive nature of the approaches.

Alternatively, skin surface electromyogram (sEMG) is a commonly used neural signal source for myoelectric control of assistive devices. sEMG can be used to determine movement intentions from muscle activity in real-time [11-13]. Myoelectric control of assistive devices is usually accomplished through pattern recognition [14] or continuous direct control methods [15]. Pattern recognition, which identifies movement patterns from predefined sets, has been used successfully to identify 19 different hand postures with a 96.7% success rate [16]. In contrast, the direct control approach enables continuous control of hand movement by mapping global EMG features, such as EMG amplitude, to kinematic or kinetic variables [15]. However, EMG amplitude is subject to interference from a variety of sources, including motion artifacts, fatigue, high background noise, as well as action potential variations; this interference may deteriorate myoelectric control performance over time [17]. More recently, deep-learning based approaches have also been implemented for motor intent detections [18-20]. Although promising, the initial training of network models is time-consuming and requires a large data set.

EMG signals consist of hundreds of motor unit action potentials (MUAPs). As an alternative to global EMG features, the motor output can also be predicted from motor unit (MU) firing activities obtained from motor unit decomposition [13, 21]. This approach estimates the neural drive input signal to the spinal motoneuron pool in the form of MU firing frequency at the population level. The time-consuming steps of the MU decomposition algorithm were circumvented in a previous study [22] by using convolutional neural networks (CNN) to derive the populational discharge frequency directly from sEMGs instead. Although the algorithm provided higher accuracy in certain cases, the internal logic of the CNN model was unknown. Previous studies have shown that the neural drive information is more robust than global EMG features in predicting finger joint kinematics [23-25], as well as fingertip

Institute of Engineering & Medicine Interdisciplinary Studies, School of Mechanical Engineering, Xi'an Jiaotong University. Xiaogang Hu (email: xxh120@psu.edu) is with the Departments of Mechanical Engineering, Kinesiology, and Physical Medicine & Rehabilitation, the Huck Institutes of the Life Sciences, and the Center for Neural Engineering at Penn State University. (correspondence e-mail: xxh120@psu.edu).

forces [26, 27], because the neural drive signal is estimated via binary neuronal firing occurrences rather than analog EMG signals. It has been demonstrated that the neural-drive method can continuously estimate forces at individual finger levels [24] and at concurrent multi-finger levels when forces vary randomly among multiple fingers [25]. Aside from finger forces, the neural-drive approach can also be used to predict joint angle during single finger oscillatory movement tasks [26, 28]. Despite the research progress, the assessment of the neuraldrive method on multi-finger dynamic movement tasks has not been explored. More importantly, dynamic joint angle estimation and fingertip force estimation were separately performed in previous studies. However, most real-world motor tasks involve complex hand activities, which include both isometric force control and dynamic movement components. performed asynchronously using multiple fingers. Therefore, it is critically important to estimate finger joint kinematics and fingertip forces concurrently across multiple fingers.

Accordingly, we developed a method based on populational MU firing activities that can concurrently estimate fingertip forces and joint angles across multiple fingers (index and middle fingers). EMG-amplitude-based prediction was also performed in parallel as a comparison. We found that the neural-drive approach outperformed the EMG-amplitude method for both finger force and joint angle estimations with a lower prediction error and a higher correlation between the estimated and recorded motor output. The developed approach could facilitate intuitive control of assistive robotic hands to perform dexterous tasks involving both force control and dynamic movement control.

# II. METHODS

An overview of the concurrent prediction of finger force and joint angle is shown in Fig. 1. We first acquired high-density EMG (HD EMG) signals of the extrinsic finger flexor and extensor muscles while participants performed isometric finger force and dynamic finger movement tasks. They performed each task using their index and middle fingers independently, and also performed both tasks sequentially using both fingers concurrently. We obtained MU firing information from the decomposition of HD EMG signals from the single finger trials. MUs were first assigned to different groups specific to each

finger and each task (isometric finger force and dynamic movement) combination. To improve decoding accuracy, the MU groups were then refined for each finger and task separately. The refined MU groups (separate matrix) were then applied directly to new HD EMG data trials in real-time involving both isometric finger force and dynamic movement tasks produced by both fingers.

# **Data Acquisition**

**Participants:** Seven healthy individuals (Age: 28±7 years) were recruited to participate in the study. No participant had any prior neuromuscular ailments. The Institutional Review Board at the University of North Carolina at Chapel Hill approved the study protocol. Prior to the experiment, all participants provided informed consent based on the approved protocols.

**Experimental Setup:** The participants were seated in a chair in front of the testing desk during the experiment. With the support of a soft foam, participants placed their right forearm on the desk in a neutral position. The experiment involved performing dynamic and isometric finger flexion using the index or middle finger. Before the experiment, the experimenter palpated the forearm to determine location of the flexor digitorum superficialis (FDS) and extensor digitorum communis (EDC) muscles in order to place the EMG electrode grid. The electrode placement was subject-specific, and was not uniform across all participants. After skin preparation, a pair of 8x16 electrode arrays were then placed on the skin over both muscles on the dorsal and volar sides of the forearm to record finger flexion-related EMG data. Each electrode of the array measured 3 mm in diameter and electrodes were spaced 10 mm apart. Using the EMG USB2+ (OT Bioelettronica) acquisition system, monopolar EMG signals were amplified with a gain of 1000, filtered (10-900Hz), and sampled at 2048 Hz. Moreover, finger force and joint angles of the index and middle fingers were measured in tandem with EMG signals for all participants. The middle and index finger movements were recorded. Two custom flex angle sensors were attached to metacarpophalangeal joints of the index and middle fingers to capture joint angle data, which were sampled at 100 Hz (Fig. 2A). To measure finger flexion forces, index and middle fingers were placed horizontally along two miniature load cells (SM-200N, Interface) mounted on the desk. The spacing and

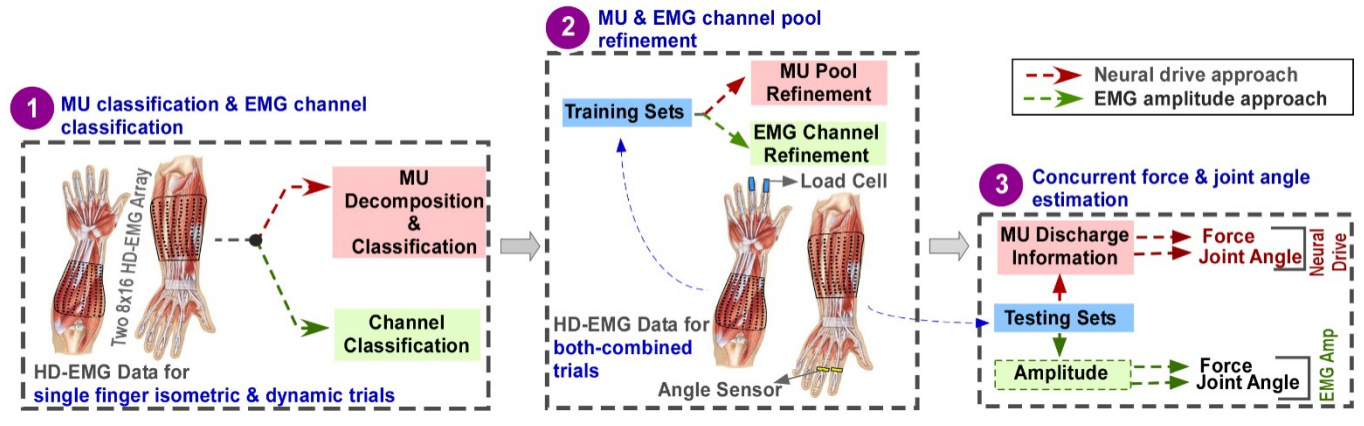


Fig 1: The method for estimating the joint angle and force concurrently for each finger from both-combined trials. Red arrows and shaded boxes point to the neural drive approach, which estimates force and joint angle concurrently based on MU firing frequency, whereas green arrows and shaded boxes indicate the traditional amplitude-based approach, which uses EMG amplitudes for estimation.

orientation of the load cells were adjustable to accommodate different hand sizes. The finger force data were sampled at 1000 Hz.

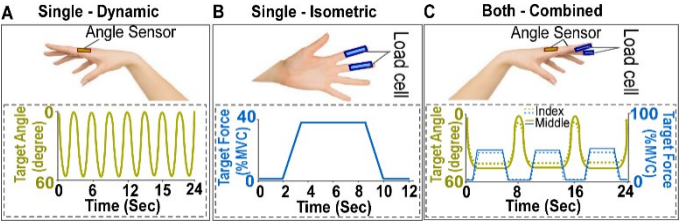


Fig 2. Experimental setup and paradigm. A) In the single finger-dynamic movement task, angle sensors were placed at the MCP joint of the index and middle fingers. Either the index or middle finger was repeatedly flexed and extended within three seconds. 60° represents full flexion and 0° represents full extension. B) During the single finger-isometric force task, two load cells were placed along the index and middle fingers to measure finger flexion forces. The participant followed a trapezoidal trajectory of 12 seconds; C) In the both finger-combined dynamic and isometric task, joint angles and flexion forces of the index and middle fingers were acquired simultaneously. After flexing both index and middle fingers from full extension, participants followed the same trapezoidal force target with both fingers, and then performed full extension.

**Experiment Procedure:** Each participant performed three different tasks in a random order using their Index and/or Middle fingers. Prior to starting the actual experiment, the data recording was examined for a short duration to disable noisy channels due to improper skin contact with electrodes. In the Single-Dynamic task, the participants were instructed to flex the MCP joints of either their index or middle finger as far as they could and then return to the full-extension position in 3 seconds (as shown in Fig. 2A). The joint angle trajectory was displayed continuously to the participants during the experiment. In a single trial of 24 seconds, the same movement was repeated eight times, and each trial was then repeated five times for each finger. A resting time of 60 seconds was provided between two successive trials. In the Single-Isometric task, the maximum voluntary contraction (MVC) of index and middle fingers was obtained separately for each participant. A trapezoidal target was then shown to the participants, and they were asked to follow the target with their index or middle finger. The trapezoid trajectory started to rise at 2 seconds, and ramped up linearly to 40% MVC. The force plateaued at 40% MVC for 8 seconds, before ramping down to 0% MVC (Fig. 2B). The participants performed the isometric force task using each finger for five trials. Similar to the previous task, a 60second rest time was provided between trials. Finger selection was randomized among the participants in both tasks. For the Both-Combined task, participants flexed both their index and middle fingers simultaneously from the full-extension position, touched the load cell, pressed against the load cell by following the same trapezoidal force target with both fingers, and moved back to the full-extension position (Fig. 2C). In a single trial, participants repeated the same activity three times within 24 seconds. The participant repeated the combined dynamic and isometric force tasks for five trials.

# Data Processing

Prior to the analysis, the HD-EMG data were preprocessed with a motion artifact removal technique [29]. Due to the significant contribution of the FDS muscle to isometric flexion force [30],

MU firing activities from the flexor EMG was used to estimate the flexion forces. The finger flexion and extension angles of individual fingers were estimated by considering both flexor and extensor muscle activations during dynamic joint movement. MU decomposition was performed on HD-EMG data obtained from the single finger isometric or dynamic tasks, and the separation matrices were then applied directly to the data from the Both-Combined trials. In parallel to the neuraldrive approach, a conventional EMG amplitude method was also performed to compare the predicted motor outputs. channel. Briefly, the data processing of both motor output prediction methods is essentially in three major steps: 1) channel optimization, 2) feature extraction (MU firing rate or EMG amplitude), and 3) estimation of the joint angle or fingertip forces. The analysis was performed entirely in MATLAB-2020b (MathWorks).

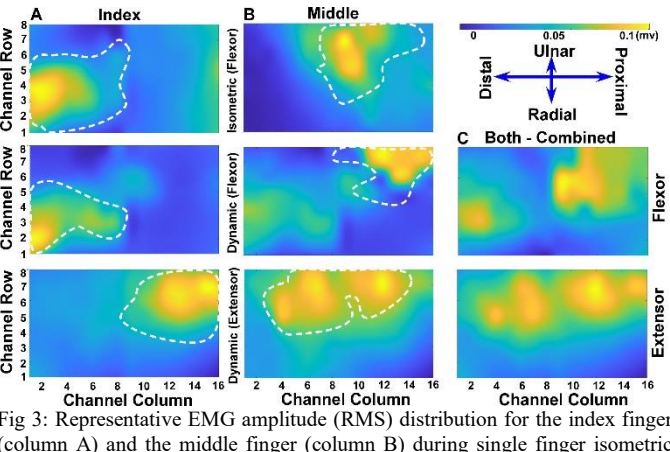


Fig 3: Representative EMG amplitude (RMS) distribution for the index finger (column A) and the middle finger (column B) during single finger isometric and dynamic trials for a single subject. In the first two rows, the amplitude distribution of flexor muscles is shown for the isometric and dynamic tasks, respectively. The last row shows the amplitude distribution of extensor muscles during dynamic finger movement. The 60 channels selected for MU decomposition are encircled by white dashed curves. The EMG-amplitude method also used the same channels to estimate the EMG amplitude for each finger. (Column C) EMG amplitude distribution for Both-Combined trials for flexion and extension.

# Motor output prediction using MU discharge information.

Channel Optimization. We observed that during the single finger isometric and dynamic tasks, muscle activation was confined to a relatively small area (Fig. 3A and Fig. 3B), while other channels exhibited relatively low EMG amplitudes. To reduce computational load, only the channels over the active area were selected for EMG decomposition. The root mean squared (RMS) amplitude was calculated for all 128 channels for this selection. These values were then averaged across the trials with the same finger and task assignments for each channel. The 60 channels with the highest RMS values were selected for decomposition. The number 60 was chosen to select approximately half of the total number of channels based on a previous study [31]. There were six sets of EMG channels: Index-Isometric-Flexor (Chiif), Middle-Isometric-Flexor Index-Dynamic-Flexor (Ch<sub>IDF</sub>), Index-Dynamic- $(Ch_{MIF}),$ Extensor (Chide), Middle-Dynamic-Flexor (Chmdf) Middle-Dynamic-Extensor (Chmde). The exemplar EMG amplitude (RMS) distribution of the Single-Isometric and

Single-Dynamic tasks are shown in Fig. 3A and Fig. 3B. Fig. 3C represents the EMG amplitude distribution of a Both-Combined trial.

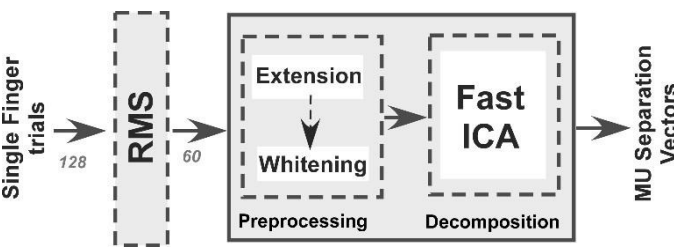


Fig 4: MU decomposition process using Fast Independent Component Analysis algorithm (FastICA).

**Feature Extraction**. This section contains information about the process of MU decomposition and MU pool formation for estimating finger force and joint angle.

**MU pool formation.** Isometric and dynamic trials for a single finger were used to obtain MU separation vectors for each finger specific to a task, and the separation vectors were combined to form a MU pool associated with that finger and task. We extracted MU firing activities using a previously developed Fast Independent Component Analysis (FastICA) algorithm [26, 32-34]. The process of MU decomposition is given in the supplementary material. The brief process of MU decomposition is illustrated in Fig. 4 (The detailed process is illustrated in Fig. S2 in the supplementary material). Briefly, the 60 selected channels were whitened and extended by a factor of (f=9). In the decomposition process, a fixed-point iteration procedure was used to obtain the separation vectors and source signals for the individual MUs. To distinguish MU discharge events (set to 1) from background signals (set to 0), the kmean++ (k=2) algorithm [35] was applied to the signals sources in order to reconstruct the binary firing events trains. Several previous studies [36, 37] have shown that ICA-based source separation can be implemented in dynamic movement conditions. The quality check at the cluster analysis stage based on Silhouette distance can also remove the inaccurate separation vectors. The separation vectors from different single finger trials of the same finger and task were combined to form a separation matrix for each finger-task combination. Separation vectors with poor separation in the cluster analysis (i.e., Silhouette values < 0.5) and duplicate MUs were removed. There were six separation matrices corresponding to six MU pools: Index-Isometric-Flexor (B<sub>IIF</sub>), Middle-Isometric-Flexor  $(B_{MIF}),$ Index-Dynamic-Flexor  $(B_{IDF}),$ Index-Dynamic-Extensor (B<sub>IDE</sub>), Middle-Dynamic-Flexor (B<sub>MDF</sub>), Middle-Dynamic-Extensor (B<sub>MDE</sub>). Fig. 5A and 5B show examples of the isometric finger force and dynamic joint angle recorded during single index finger trials. The corresponding MU firing event trains are shown in Fig. 5C and 5D, respectively. Similarly, irregular variations in joint angle was also evident in Fig. 5D. This overestimation of neural drive signals may result from the inclusion of MUs related to different finger-task combinations, due to inevitable co-activation of other undesired fingers. The HD EMG grid covers a majority of the multicompartment muscles and MU action potentials from different compartments can be registered concurrently.

decomposition algorithm could not distinguish which MUs belong to which finger.

**MU pool refinement.** A MU pool refinement procedure was implemented to eliminate MUs related to either use of an undesired finger or performance of an incorrect task while retaining MUs that were pertinent to the selected task-finger combination. EMG data from Both-Combined trials were used for this process. We divided the Both-Combined trials into two groups: training and testing. Training data were used to refine the MU pool, whereas Testing data were used to estimate forces and joint angles. We performed a five-fold cross-validation, in which four groups were used for training, and the remaining group was used for testing. A two-step refinement process was performed in this study:

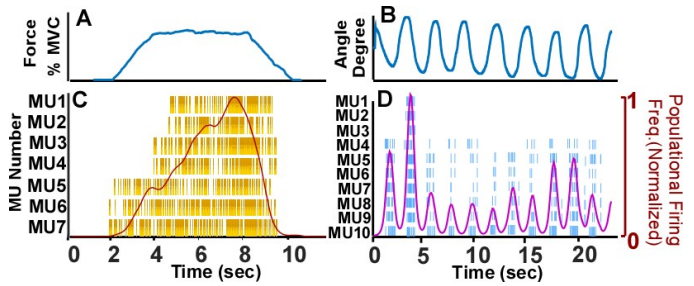


Fig 5: Extracted MU firing information from single-finger trials. Exemplar isometric force (A) and dynamic movement (B) trials of the single-finger (index) tasks. MU firing event trains of a single-isometric trial (C) associated with the finger forces (A). A single-dynamic trial (D) associated with the joint angle (B). The red curve shows the populational MU firing frequency.

- **Task-Based Refinement:** Some MUs may be preferentially activated during dynamic movement, while other MUs may be more active during isometric force production. In the task-based refinement, MUs more related to dynamic tasks were removed from the MU pool corresponding to isometric tasks of the same finger, and vice versa. The rationale was that the firing rate of some MUs may be better correlated with forces than with dynamic joint angles, and vice versa. In this refinement process, we applied the MU pools obtained from the previous steps to the EMG data of the Both-Combined trials (training set) and calculated the individual MU firing rate by averaging values across a 0.5-s average window with a step size of 0.1-seconds (the same window was used throughout the study). The recorded force and joint angle of the targeted finger were also processed over the same window. A firstorder linear regression was performed between the MU firing rate and the isometric force of the targeted finger, whereas a second-order linear regression was performed between the MU firing rate and the joint angle of intended finger [26]. MUs were retained if the coefficient of determination (R<sup>2</sup>) value was higher for the desired task than for the other task; otherwise, the MUs were discarded. The regression analysis and R<sup>2</sup> comparisons were conducted on all the MUs during the refinement. A taskbased refinement example for the Index-Isometric-Flexor MU pool (B<sub>IIF</sub>) is shown in the Supplementary Material.
- Finger-Based Refinement: The close proximity of individual finger muscles could cause interference in single-finger muscle activity due to co-contraction of

adjacent muscle compartments. To remove the MUs related to other fingers, a finger-based refinement procedure [31] was performed after the task-based refinement. During the combined trials, both fingers carried out simultaneous tasks, but their actual force or kinematic profiles were slightly different. For example, different fingers may touch the load cells at different timings, and rate of rise of the force profiles can be different. These distinct features across fingers allowed us to separate the MUs into finger-specific groups. Specifically, MUs retained after the task-based refinement were applied to the Both-Combined trial to determine the firing rates of individual MUs. Force and joint angle data from the index and middle fingers were smoothed using the same average window. For the isometric MU pools, the finger-based refinement was performed using the firstorder linear regression between MU firing rate and individual finger force, while for the dynamic MU pools, a second-order linear regression was used between MU firing rate and finger joint angles. If the targeted finger had a higher R<sup>2</sup> than the other finger, the MU was kept; otherwise, the MU was removed from the MU pool. The Supplementary Material shows an example of finger-based refinement for the Index-Isometric-Flexor MU pool (B<sub>IIF</sub>).

The average number of MUs in the individual MU pools after refinement is summarized in Table S1 (in supplementary material). Each condition averaged between 21-51 MUs that were ultimately used for analysis. The high number of MUs used to calculate the source signal may also result in an increase in computational complexity and delay during force and joint angle estimation. Alternatively, N number of MUs from each of the MU pools were selected to predict finger forces and joint movements of the testing trials. We derived MU separation vectors from single-finger trials and then applied them to multifinger trials for estimating force and joint angle. It is possible that the testing trials might contain a small number of MU spike trains. Therefore, we selected a smaller number of MUs for the testing trials such that at least those MUs would appear in those test trials. In our preliminary investigation, it appears that, rather than using populational firing frequency of all MUs, we can also use individual firing activities of a small number of MUs for an accurate estimation of forces and joint angles [26]. According to our pilot evaluation, N=5 was selected as a reasonable choice. The MUs were selected based on the R2 value obtained through a regression between the firing frequency and force (in case of isometric MU pool) or joint angle (in case of dynamic MU pool) when individual MU separation vectors were applied to a different Both-Combined training trial. The 5 MUs with the highest R<sup>2</sup> values were then selected.

#### Finger force and Joint angle estimation.

**Finger force estimation.** The selected five isometric MUs for individual fingers were directly applied to the EMG data of the Both-Combined trials (testing). The firing frequency of each MU was calculated using an average window of 0.5 seconds and moving step of 0.1 second. A Kalman filter (the system matrix = 1, the observation matrix = 1, the system covariance =

0.1 and the observation covariance = 0.5) was then applied to the firing frequency to eliminate isolated and sporadic fluctuations. At the same time, the finger force data for both fingers were smoothed with the same window. The firing rate of all five MUs and the force of the targeted finger  $(F_i)$  were fit into a multivariate linear model to predict finger forces (Eq. 1):

$$F_i(t) = \sum_{j=1}^5 a_{i,j} D_{i,j}(t) + b_i$$
 (1)

where,  $F_i$ =force of the *i*-th finger (i = index or middle); j=index of MUs; D = Firing rate of MUs; t=time;  $a_i$  and  $b_i$ =regression coefficients [38].

**Joint Angle estimation.** The dynamic MU pools for both the flexors and extensors were applied directly to the testing trials, and the obtained firing frequencies of all the MUs (after processing with the average window and Kalman filter) were then fit into a multivariate model using the smoothed joint angle value (using the same average window) recorded for the targeted finger (Eq. 2):

$$JA_{i}(t) = \sum_{MU_{f}=1}^{5} (P_{i,MU_{f}} D_{f,i,MU_{f}}(t) + Q_{i,MU_{f}} D_{f,i,MU_{f}}^{2}(t)) + terms for Flexor MUs$$

$$\sum_{MU_{e}=1}^{5} (R_{i,MU_{e}} D_{e,i,MU_{e}}(t) + S_{i,MU_{e}} D_{e,i,MU_{e}}^{2}(t)) + C_{i}$$

$$terms for Extensor MUs$$
(2)

where,  $JA_i$  =joint angle of the *i*-th finger (i = index or middle);  $MU_f$  &  $MU_e$  =number of flexor & extensor MUs, respectively;  $D_f$  &  $D_e$  =firing rate of flexor and extensor MUs;  $P_i$ ,  $Q_i$ ,  $R_i$ ,  $S_i$ , and  $C_i$ =regression coefficients.

#### Motor output prediction using EMG amplitude.

Channel Optimization and Feature Extraction. EMG amplitude-based force and joint angle estimation were also performed. From Fig. 3A and 3B, it was evident that even though the 60 selected channels covered the most active regions for specific finger-task combinations, there were considerable overlaps between the isometric and dynamic tasks performed with the same finger. In addition, substantial overlap in activation between finger muscles was observed while performing the single-finger task. Accordingly, task-based and finger-based refinement approaches were carried out to refine the EMG channel sets for each finger-task combination. Data from Both-Combined training trials were used for this refinement. The EMG amplitudes (RMS) of the individual channels were calculated by performing a moving average across a window of 0.5 seconds and moving step of 0.1 second. In the task-based refinement, the R<sup>2</sup> values from the regression of the EMG amplitude and force were compared with those obtained from the regression of the same EMG amplitude and the joint angle of the same finger. For the isometric channel pools, the EMG channel was retained, if the R<sup>2</sup> value was higher in the force regression. For the dynamic channel pools, the channel was retained, if the R<sup>2</sup> value was higher in the angle regression. A similar finger-based refinement was performed on the remaining EMG channels. The supplementary Figure S1 shows an example of task-based refinement on the EMG channel pool of Index-Isometric-Flexor (Chiif).

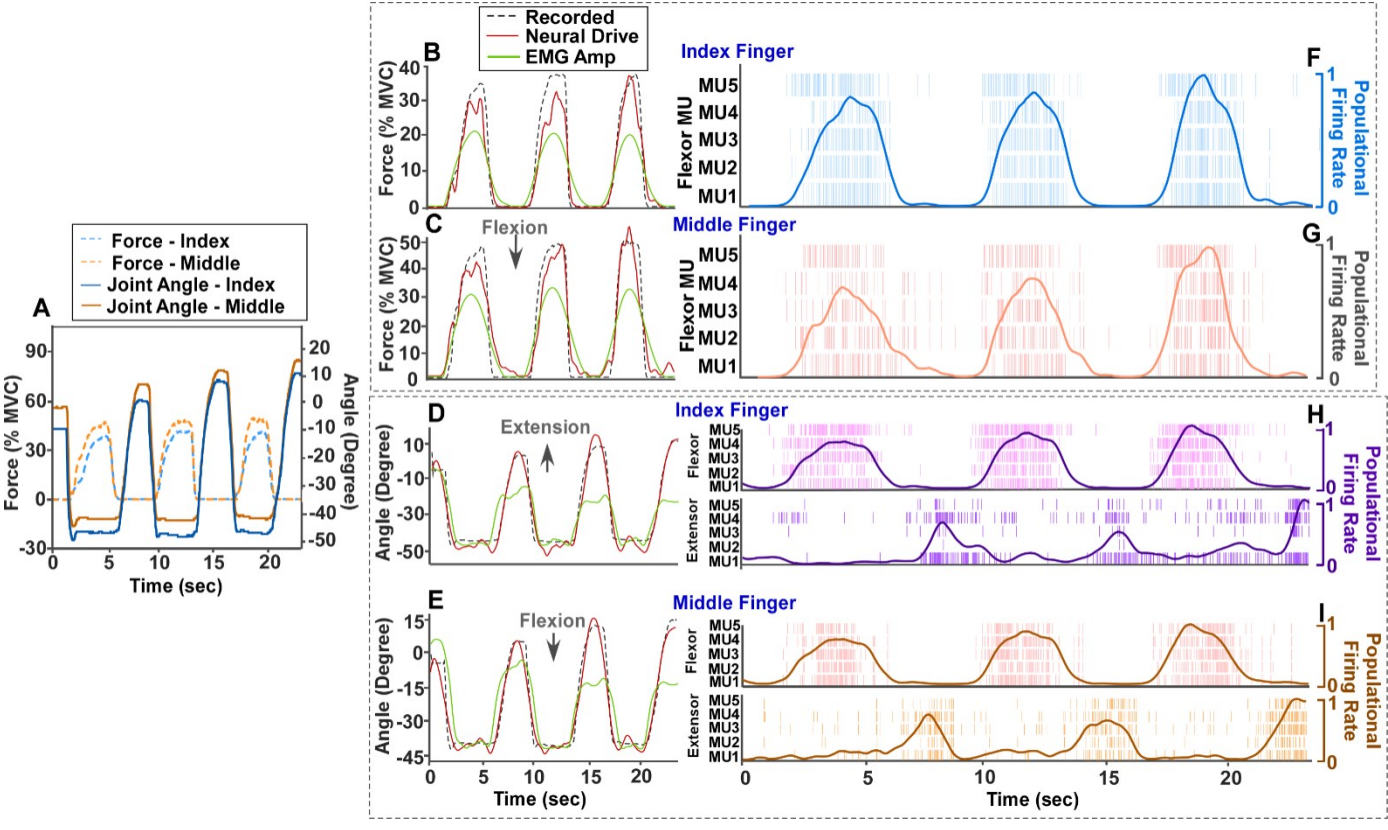


Fig 6: A representative example of a Both-Combined test trial with simultaneous recording of index and middle finger forces and joint angles (A); The concurrent estimation of force (B &C) and joint angle (D & E) for individual fingers using the neural-drive and EMG-amplitude methods. MU firing event trains and populational firing frequency associated with the estimation of force (F & G) and joint angle (H & I) of individual fingers.

Finger force and joint angle estimation. Evaluation of the EMG-amplitude method on force and joint angle estimation was performed on the Both-Combined testing trials. EMG amplitudes (RMS) of the refined channel pools using the same average window was calculated, followed by an average across EMG channels. The same Kalman filter was applied. For force prediction, the overall EMG amplitude was fit into a linear model using forces of the targeted finger (Eq. 3):

$$F_i(t) = c_i A_i(t) + d_i \tag{3}$$

where,  $F_i$  =force of the *i*-th finger (i = index or middle);  $A_i$ =RMS of EMG;  $c_i$  and  $d_i$ =Regression coefficients.

To predict joint angles, the amplitudes of both the flexor and extensor were fit into a bivariate linear model using the joint angle of the target finger (Eq. 4):

$$JA_{i}(t) = u_{i}A_{f,i}^{2}(t) + v_{i}A_{e,i}^{2}(t) + x_{i}A_{f,i}(t) + y_{i}A_{e,i}(t) + z_{i}$$
(4)

where,  $JA_i$  = Joint angle of the *i*-th finger (i = index or middle);  $A_f$  &  $A_e$  = RMS for Flexor and Extensor;  $u_i$ ,  $v_i$   $x_i$ ,  $y_i$  and  $z_i$ =Regression coefficients.

#### **Statistical Analysis**

The accuracy of the neural-drive and EMG-amplitude methods on force and joint angle prediction was evaluated using the root mean square error (RMSE) and R<sup>2</sup> value. For individual fingers, the R<sup>2</sup> and RMSE values were averaged across trials and across participants to represent the overall performance. Data distribution for the obtained RMSE and R<sup>2</sup> values were checked using the Kolmogorov-Smirnov test. As these were normally distributed, paired t-tests were used to compare the performance between methods. The t-test was performed for the same finger across all participants. A Bonferroni-Holm adjustment was performed to avoid Type-I errors that can result from multiple t-tests.

#### III. RESULTS

## A. Performance for Force estimation

Fig. 6 shows the predicted output of a representative Both-Combined test trial. A comparison of the force estimation from this trial using neural-drive and EMG-amplitude methods is illustrated in Fig. 6B and 6C. The MU firing event trains of the index and middle finger flexor and extensor muscles used for the neural drive calculation are shown in Fig. 6F and 6G, respectively. An alternating MU firing activity between the flexor and extensor muscles are evident.

We then quantified the force prediction performance using RMSE and  $R^2$  between the recorded and the predicted force using the neural-drive and EMG-amplitude methods (Fig. 7A and 7B). The neural-drive method showed a lower estimation error for both index (RMSE=3.47±0.43 %MVC (mean ± standard error)) and middle (RMSE=4.47±0.82 %MVC) fingers, when compared with the EMG-amplitude method

(index: RMSE=6.64±0.69 %MVC; middle: RMSE=9.73±1.04 %MVC). A significant difference between the two methods was identified using t-tests with Bonferroni-Holm adjusted p level of 0.025 (index: t = -4.86, p = 0.0028, Cohen's d = -2.07; middle: t = -4.02, p = 0.0069, Cohen's d = -2.16). Similarly, the neural-drive estimated force had a higher correlation with the recorded finger force (Fig. 7B). Namely, the median value for the neural-drive method (index:  $R^2$ =0.77 and middle:  $R^2$ =0.73) was higher than that of the EMG-amplitude method (index:  $R^2$ =0.71 and middle:  $R^2$ =0.61). A significant difference was observed (index: t = 3.08, p = 0.0082, Cohen's t = 2.37; middle: t = 3.80, t = 0.0089, Cohen's t = 2.12).

#### B. Performance for Joint Angle estimation.

For the Both-Combined test trials, the joint angle estimated by the neural-drive method closely resembles the measured joint angle, whereas the EMG-amplitude method showed an underestimation on the predicted angles (Fig. 6D and 6E). The MU firing event trains of the extensor and flexor muscles of the index and middle fingers are shown in Fig. 6H and 6I, respectively.

We also evaluated the joint angle prediction performance of the neural-drive and EMG-amplitude methods, using the RMSE and R<sup>2</sup> from the Both-Combined test trials (Fig. 7C and 7D). Paired *t*-test results on the RMSE values indicated that the neural-drive method has a significantly smaller angle estimation error than the EMG-amplitude method (index: t = -6.21, p = 0.0054, Cohen's d = -4.88; middle: t = -5.30, p = 0.0018, Cohen's d = -2.55). Similarly, the *t*-test of R<sup>2</sup> values showed that the neural drive approach has a higher correlation with the measured joint angle than the EMG-amplitude method (index: t = 8.17, p = 0.0047, Cohen's d = 4.32; middle: t = 6.86, p = 0.0018, Cohen's d = 3.71). Specifically, we found a smaller angle estimation error of the neural-drive approach (index:

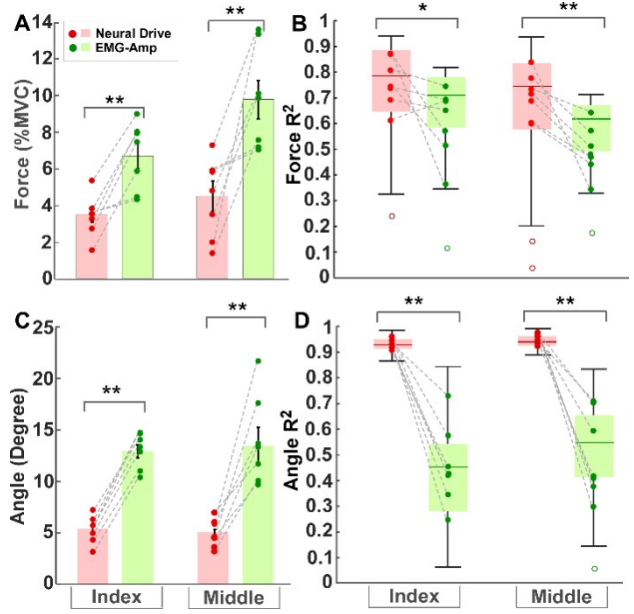


Fig 7: The RMSE (A & C) and the R2 value (B & D) of the neural-drive and EMG-amp methods of all the participants. The individual circles represent the RMSE and R2 value of individual participants. The same participants are connected in dash lines. \*, p < 0.05. \*\*, p < 0.01.

RMSE=5.40±0.50°; middle: RMSE=5.00±0.49°) than the EMG-amplitude method (index: RMSE=12.8±0.65°; middle: RMSE=13.4±1.74°). The neural-drive method also showed a higher angle correlation for both fingers (index:  $R^2$ =0.93 and middle:  $R^2$ =0.94) than the EMG-amplitude method (index:  $R^2$ =0.45 and middle:  $R^2$ =0.54). Further, a *post-hoc* test using Bonferroni-Holm corrections (adjusted *p* level of .0025) showed significantly lower estimation errors (RMSE) and higher correlation ( $R^2$ ) for both index and middle finger joint angle estimations of the neural-drive method.

#### IV. DISCUSSION

The purpose of our study was to develop a neural decoding method based on motoneuron firing information obtained from HD-EMG signals of extrinsic finger muscles. This approach could concurrently estimate joint kinematics and kinetics of multiple fingers, while participants performed multi-finger isometric force and dynamic movement tasks together. Our results showed that the neural-drive method performed significantly better than the conventional EMG amplitudebased method in terms of force and joint angle estimation, with a smaller prediction error and a higher correlation with the measured motor output. These findings demonstrated that the developed approach is potentially suitable for continuous interface with assistive robotic hands at individual finger levels. The outcomes show that the neural decoding approach has the potential to enable dexterous motor control of assistive devices during daily motor tasks.

The main contribution of the current work is the development of a neural decoder that can concurrently predict isometric forces and dynamic joint kinematics at individual finger levels. In previous literature [24-26, 28], MU firing information has been used to estimate fingertip forces and joint angles of individual fingers in separate studies. Specifically, MUs are decomposed from HD EMG data, and the neural drive signals can be estimated by populational MU firing activity. Different regression functions are then adopted to map the estimated neural derive signals to either forces or joint angles. However, in most daily activities, our hands perform force-based control tasks as well as dynamic movement tasks together using multiple fingers. Therefore, to meet every day needs with assistive robotic hands, it is necessary to determine both finger force and joint angle at the same time for individual fingers. Based on our study, different sets of MUs can be preferentially activated for kinematic and kinetic control tasks, which is consistent with earlier studies showing that different cortical neurons are involved in kinematic and kinetic control [39] and that the learning processes between the two tasks are also somewhat independent [40]. As a result, the earlier neural decoders based on kinematic or kinetic variables may not be generalizable to the other variables. The currently developed decoder directly addresses this issue by constructing task- and finger-specific MU groups for the estimation of neural drive signals. All these calculations were performed offline because of high-computational intensity. After these calculation steps are completed, we can reuse these matrices for subsequent realtime calculations.

Decomposition of EMG signals into MUs is time-consuming, which poses a challenge for real-time neural-machine interface. A few studies have implemented the idea of real-time decomposition by pre-calculating separation vectors using a small data set, and the neural drive can then be derived by applying the separation matrix directly to a new data set [26, 41]. This protocol requires a time-consuming decomposition step each time before being applied to motor output estimation in real-time for a new data-set. Instead, in the current study, MU decomposition was performed separately using data from the single-finger isometric force and dynamic movement tasks. MUs from the same finger and task were clustered to form an initial pool of MUs corresponding to the particular finger label and particular task label. These subgroups of MUs were then refined to improve decoding accuracy. Previous studies have explored a finger-based refinement procedure for MU pools [24, 25] to eliminate MUs resulting from co-activation of unintended fingers. An additional task-based refinement procedure was performed in the current study to retain MUs that are more relevant to the specific task of a given finger. We then applied these sets of MUs directly to a new dataset to estimate force and joint angle for both fingers concurrently. This procedure allows concurrent task- and finger-specific motor decoding in a real-time manner. Since the MU pools were formed for each finger-task combination, we can reuse them for more complex finger movement without re-running the time-consuming MU decomposition steps.

We estimated both isometric force and dynamic joint angle using MU firing information. As a comparison, implemented the traditional EMG amplitude method to estimate individual finger forces and joint angles. For fair comparison, we also performed channel refinement to retain EMG channels with high signal quality and minimally interfered by cross-talk. Prior studies showed that neural drive approaches were more accurate in terms of RMSE and R<sup>2</sup> value for individual finger force prediction, during both single and multi-finger tasks [24, 25]. We also observed large force underestimations in the EMG amplitude method compared with the neural-drive method when both index and middle fingers jointly performed the task. Detailed results also showed that the neural drive method performed better for individual participants than the EMG amplitude method. Similarly, when correlated with the ground truth, higher R<sup>2</sup> values were observed using the neural-drive predicted force than the EMG-amplitude predicted forces. These results demonstrate that the estimated force for the index and middle fingers using the neural drive method is more reliable than the EMG amplitude method for estimating finger force, because the neural-drive method based on MU firings are not sensitive to EMG amplitude interference over time.

Regarding joint angle estimation, the estimation performance of the neural drive method is considerably higher than the EMG amplitude method at the individual participant level, which implies that the EMG amplitude method might not be suitable for estimating joint kinematics for individual fingers during complex hand movements. Previous studies have also found similar results for single finger joint angle estimation [28]. The

large error in joint angle estimation may be caused by a variety of intrinsic and extrinsic factors, such as changes in relative position between EMG electrodes and muscle compartments, large motion artefact, varying background noise, that can bias EMG amplitude estimation. In our study, a motion artifact removal method [29] was applied to the EMG signals before the EMG amplitude calculation. We expect an even higher estimation error of the EMG amplitude method without this artefact removal step. In contrast, angle estimation via the neural drive method is based on binary spikes trains, which is less likely to be affected by the interference factors.

The current study also has several limitations. To estimate flexion forces of individual fingers, only MUs of the flexors were used to calculate the neural drive signals. Our experimental designlimited finger extension force measurement, because the task involved a motor sequence: finger flexion, touch the load cells, apply force on the load cell, and finger extension. Nevertheless, the low prediction error using the neural-drive approach indicated that only the flexor MUs were sufficient to estimate isometric finger force. Moreover, the results demonstrated that the selected first-order regression model was able to predict the measured forces accurately. However, underestimation or overestimation was observed near the peak values (refer Fig. 6B & Fig. 6C) of the predicted forces, perhaps because of a lack of consideration of co-activated extensor MUs. Future studies will include the extensor MUs in the neural drive calculation to evaluate whether the force prediction performance can be further improved. During prolonged muscle activation, stationarities in EMG signals can reduce the validity of previously calculated separation matrices. Our current study did not address this important issue. To maintain the validity of the separation matrix, a periodic update mechanism of the separation matrix is needed. In a previous study [42], we developed a double-thread decomposition technique to address changes of EMG signals due to drift of action potential amplitude, varying background noise level, and sporadic motor unit recruitment and de-recruitment patterns. The back-end thread performs the computationally intensive separation matrix calculation and matrix refinement (which is equivalent to the offline initialization process), and the updated separation matrix can be fed to the front-end thread periodically for realtime decomposition. It is possible to implement the separation matrix refinement procedures in the current study to the backend thread to accommodate EMG non-stationarities. In the current study, simple linear regression models were used to estimate joint and force firing rates without taking into account different contributions from individual MUs. In addition, only a subset of five MU firing activities were utilized for the motor output predictions. The choice of the regression functions and the number of MUs were indeed largely arbitrary. In future studies, it is necessary to identify the optimal regression functions and the optimal number of MUs for moto output predictions. Lastly, during daily activities it is possible that both fingertip forces and joint angles vary concurrently (e.g., squeezing a soft object). Whether we should use the force related MUs or angle related MUs will depend on the control policy we specify. If we activate the force controller once force (above a threshold) is registered on the finger force sensor, then

the force related MUs will be used to control the fingertip force regardless the finger joint is moving or not. Nevertheless, further studies are needed to specifically evaluate this issue. We also plan to further evaluate asynchronized motor output variations among fingers, such as some fingers produced force output while others produced dynamic movement, or different fingers produced different levels of forces. Since the MUs were specific to individual fingers and specific to different tasks following the refinement procedure, we expect that the same set of MUs can be used to estimate finger motor output correctly when different fingers engage in different tasks.

#### V. CONCLUSION

This study developed a neural decoding method for simultaneous estimation of finger forces and joint angles of individual fingers during complex hand movements involving a combination of dynamic motions and isometric forces. As an alternative to the traditional EMG amplitude-based method, we used the MU firing information to obtain finger-specific and task-specific neural control signals and to minimize the impact of intrinsic and extrinsic interference on the motor output estimation. Our findings indicate that it is possible to predict the finger force and joint angle together for individual fingers using MU firing activities. Through further improvement of this method, a robust human-machine interface could be implemented to allow highly dexterous, individual finger movements of assistive robotic hands.

#### **REFERENCES**

- [1] A. Calado, F. Soares, and D. Matos, "A review on commercially available anthropomorphic myoelectric prosthetic hands, pattern-recognition-based microcontrollers and sEMG sensors used for prosthetic control," pp. 1-6: IEEE.
- [2] M. Ghassemi and D. G. Kamper, "A Hand Exoskeleton for Stroke Survivors' Activities of Daily Life," pp. 6734-6737: IEEE.
- [3] J. Vertongen and D. Kamper, "Design of a 3D printed hybrid mechanical structure for a hand exoskeleton," *Current Directions in Biomedical Engineering*, vol. 6, no. 2, 2020.
- [4] P. D. E. Baniqued *et al.*, "Brain–computer interface robotics for hand rehabilitation after stroke: A systematic review," *Journal of neuroengineering and rehabilitation,* vol. 18, no. 1, pp. 1-25, 2021.
- [5] L. Bi and C. Guan, "A review on EMG-based motor intention prediction of continuous human upper limb motion for humanrobot collaboration," *Biomedical Signal Processing and Control*, vol. 51, pp. 113-127, 2019.
- [6] S. Lee and C. Lee, "Toward advanced neural interfaces for the peripheral nervous system (PNS) and their future applications," *Current Opinion in Biomedical Engineering*, vol. 6, pp. 130-137, 2018.
- [7] K. Volkova, M. A. Lebedev, A. Kaplan, and A. Ossadtchi, "Decoding movement from electrocorticographic activity: a review," *Frontiers in neuroinformatics*, vol. 13, p. 74, 2019.
- [8] M. Simão, N. Mendes, O. Gibaru, and P. Neto, "A Review on Electromyography Decoding and Pattern Recognition for Human-Machine Interaction," *IEEE Access*, vol. 7, pp. 39564-39582, 2019.
- [9] L. Yao, B. Zhu, and M. Shoaran, "Fast and accurate decoding of finger movements from ECoG through Riemannian features

- and modern machine learning techniques," *Journal of Neural Engineering*, vol. 19, no. 1, Art. no. 016037, 2022.
- [10] Z. T. Irwin et al., "Neural control of finger movement via intracortical brain-machine interface," *Journal of neural* engineering, vol. 14, no. 6, Art. no. 066004, 2017.
- [11] J. Liu, Y. Ren, D. Xu, S. H. Kang, and L.-Q. Zhang, "EMG-based real-time linear-nonlinear cascade regression decoding of shoulder, elbow, and wrist movements in able-bodied persons and stroke survivors," *IEEE Transactions on Biomedical Engineering*, vol. 67, no. 5, pp. 1272-1281, 2019.
- [12] N. Parajuli et al., "Real-time EMG based pattern recognition control for hand prostheses: A review on existing methods, challenges and future implementation," Sensors, vol. 19, no. 20, p. 4596, 2019.
- [13] D. Farina et al., "The extraction of neural information from the surface EMG for the control of upper-limb prostheses: emerging avenues and challenges," *IEEE Transactions on Neural Systems and Rehabilitation Engineering*, vol. 22, no. 4, pp. 797-809, 2014.
- [14] A. J. Young, L. H. Smith, E. J. Rouse, and L. J. Hargrove, "Classification of Simultaneous Movements Using Surface EMG Pattern Recognition," *IEEE Transactions on Biomedical Engineering*, vol. 60, no. 5, pp. 1250-1258, 2013.
- [15] C. Dai, Y. Zheng, and X. Hu, "Estimation of Muscle Force based on Neural Drive in a Hemispheric Stroke Survivor," Frontiers in Neurology, vol. 9, 2018, Art. no. 187.
- [16] A. A. Adewuyi, L. J. Hargrove, and T. A. Kuiken, "An analysis of intrinsic and extrinsic hand muscle EMG for improved pattern recognition control," *IEEE Transactions on Neural Systems and Rehabilitation Engineering*, vol. 24, no. 4, pp. 485-494, 2015.
- [17] T. Moritani, M. Muro, and A. Nagata, "Intramuscular and surface electromyogram changes during muscle fatigue," *Journal of Applied Physiology*, vol. 60, no. 4, pp. 1179-1185, 1986.
- [18] P. Xia, J. Hu, and Y. Peng, "EMG-Based Estimation of Limb Movement Using Deep Learning With Recurrent Convolutional Neural Networks," *Artificial Organs*, vol. 42, no. 5, pp. E67-E77, 2018.
- [19] T. Bao, S. A. R. Zaidi, S. Xie, P. Yang, and Z.-Q. Zhang, "A CNN-LSTM Hybrid Model for Wrist Kinematics Estimation Using Surface Electromyography," *IEEE Transactions on Instrumentation and Measurement*, vol. 70, pp. 1-9, 2021.
- [20] G. Hajian and E. Morin, "Deep Multi-Scale Fusion of Convolutional Neural Networks for EMG-Based Movement Estimation," *IEEE Transactions on Neural Systems and Rehabilitation Engineering*, vol. 30, pp. 486-495, 2022.
- [21] A. Caillet, A. T. M. Phillips, D. Farina, and L. Modenese, "Estimation of the firing behaviour of a complete motoneuron pool by combining EMG signal decomposition and realistic motoneuron modelling," bioRxiv, 2022.
- [22] R. Roy, F. Xu, D. G. Kamper, and X. Hu, "A generic neural network model to estimate populational neural activity for robust neural decoding," *Computers in Biology and Medicine*, vol. 144, Art. no. 105359, 2022.
- [23] C. Dai, Y. Cao, and X. Hu, "Prediction of individual finger forces based on decoded motoneuron activities," *Annals of biomedical engineering*, vol. 47, no. 6, pp. 1357-1368, 2019.
- [24] Y. Zheng and X. Hu, "Concurrent Estimation of Finger Flexion and Extension Forces Using Motoneuron Discharge Information," *IEEE Transactions on Biomedical Engineering*, vol. 68, no. 5, pp. 1638-1645, 2021.
- [25] Y. Zheng and X. Hu, "Concurrent Prediction of Finger Forces Based on Source Separation and Classification of Neuron Discharge Information," *International Journal of Neural Systems*, vol. 31, no. 06, Art. no. 2150010, 2021.

- [26] F. Xu, Y. Zheng, and X. Hu, "Estimation of Joint Kinematics and Fingertip Forces using Motoneuron Firing Activities: A Preliminary Report," in 2021 10th International IEEE/EMBS Conference on Neural Engineering (NER), 2021, pp. 1035-1038. 2021.
- [27] N. Rubin, Y. Zheng, H. Huang, and X. Hu, "Finger Force Estimation Using Motor Unit Discharges Across Forearm Postures," *IEEE Transactions on Biomedical Engineering*, vol. 69, no. 9, pp. 2767-2775, 2022.
- [28] C. Dai and X. Hu, "Finger joint angle estimation based on motoneuron discharge activities," *IEEE Journal of Biomedical* and Health Informatics, vol. 24, no. 3, pp. 760-767, 2019.
- [29] Y. Zheng and X. Hu, "Interference Removal From Electromyography Based on Independent Component Analysis," *IEEE Transactions on Neural Systems and Rehabilitation Engineering*, vol. 27, no. 5, pp. 887-894, 2019.
- [30] Z. M. Li, V. M. Zatsiorsky, and M. L. Latash, "The effect of finger extensor mechanism on the flexor force during isometric tasks," *Journal of Biomechanics*, vol. 34, no. 8, pp. 1097-1102, 2001/08/01/2001.
- [31] Y. Zheng and X. Hu, "Concurrent Estimation of Finger Flexion and Extension Forces Using Motoneuron Discharge Information," *IEEE Trans Biomed Eng*, vol. 68, no. 5, pp. 1638-1645, May 2021.
- [32] C. Dai and X. Hu, "Independent component analysis based algorithms for high-density electromyogram decomposition: Experimental evaluation of upper extremity muscles," *Comput Biol Med*, vol. 108, pp. 42-48, 2019.
- [33] C. Dai and X. Hu, "Independent component analysis based algorithms for high-density electromyogram decomposition: Systematic evaluation through simulation," *Comput Biol Med*, vol. 109, pp. 171-181, 2019.
- [34] M. Chen and P. Zhou, "A Novel Framework Based on FastICA for High Density Surface EMG Decomposition," *IEEE Trans Neural Syst Rehabil Eng*, vol. 24, no. 1, pp. 117-27, 2016.
- [35] Y. Ning, X. Zhu, S. Zhu, and Y. Zhang, "Surface EMG decomposition based on K-means clustering and convolution kernel compensation," *IEEE J Biomed Health Inform*, vol. 19, no. 2, pp. 471-7, 2015.
- [36] V. Glaser and A. Holobar, "Motor Unit Identification From High-Density Surface Electromyograms in Repeated Dynamic Muscle Contractions," *IEEE Transactions on Neural Systems* and Rehabilitation Engineering, vol. 27, no. 1, pp. 66-75, 2019.
- [37] C. Dai, Y. Cao, and X. Hu, "Estimation of Finger Joint Angle Based on Neural Drive Extracted from High-Density Electromyography," Annu Int Conf IEEE Eng Med Biol Soc, vol. 2018, pp. 4820-4823, Jul 2018.
- [38] N. R. Draper and H. Smith, *Applied regression analysis*. John Wiley & Sons, 1998.
- [39] M. P. Branco, L. M. de Boer, N. F. Ramsey, and M. J. Vansteensel, "Encoding of kinetic and kinematic movement parameters in the sensorimotor cortex: A Brain-Computer Interface perspective," *European Journal of Neuroscience*, vol. 50, no. 5, pp. 2755-2772, 2019.
- [40] Q. Fu, W. Zhang, and M. Santello, "Anticipatory planning and control of grasp positions and forces for dexterous two-digit manipulation," *Journal of Neuroscience*, vol. 30, no. 27, pp. 9117-9126, 2010.
- [41] Y. Zheng and X. Hu, "Real-time isometric finger extension force estimation based on motor unit discharge information," *Journal of Neural Engineering*, vol. 16, no. 6, Art. no. 066006, 2019.
- [42] Y. Zheng and X. Hu, "Adaptive Real-Time Decomposition of Electromyogram During Sustained Muscle Activation: A Simulation Study," *IEEE Transactions on Biomedical Engineering*, vol. 69, no. 2, pp. 645-653, 2022.